that it should be quite useful in several cases. However, it is clearly necessary to do further work in order to find out the limitations of this method. It would be desirable to study a greater variety of geometries as well as investigating the theoretical aspects of the problem more in detail.

The author is greatly indebted to Mr. M. Leimdörfer, A. B. Atomenergi, Stockholm, for communicating his results prior to publication and for interesting discussion.

REFERENCES

1. H. Goldstein, "Fundamental Aspects of Reactor Shielding." Addison-Wesley, Reading, Massachusetts, 1959.
2. M. Leimdörfer, to be published.
3. B. Carlson, The Monte Carlo method applied to a problem in γ-ray diffusion. AECU-2857 (1953).

Sven A. E. Johansson

Department of Physics
University of Lund
Lund, Sweden

Received December 27, 1961
Revised July 12, 1962

Two Regimes of Burnout (DNB) Correlated with Steam Energy Flow for Uniformly-Heated Channels

Experimental determinations of "burnout heat flux" in subcooled or boiling-water systems have generally been supplanted by measurements which determine the heat flux at which nucleate boiling has become intense enough to start formation of a low-conductivity film of steam on the surface. The phenomenon is frequently called "departure from nucleate boiling" (DNB), and is usually considered to occur at heat fluxes only a few percent below those causing physical burnout and destruction of the test element. When published values of DNB heat-flux are plotted against such arguments as quality (x), enthalpy (h), or mass velocity (G) the data show wide scatter.

This scatter is minimized when the data are plotted against the argument $G(h - h_{\text{saturation}})$, which has the same dimensions as heat flux, Btu/ft² hr or watts/cm². In a boiling channel $G(h - h_f)$ can be called "steam energy flow" or "SEF" and signifies the rate of flow of enthalpy of vaporization across unit flow area. Its value at the core exit is a measure of boiling reactor performance, and depends only upon the flow of feedwater which is totally vaporized in the core, not upon any accompanying recirculating saturated-water flow used as a "carrier" for the feedwater.

$G(h - h_{fg})$ has a negative value for subcooled water, and is a convenient correlating parameter in the subcooled region also. The use of negative values of steam energy flow is analogous to the use of "negative quality" ($x < 0$) in other correlations.

Figure 1 is a typical plot of DNB heat flux against SEF with uniform axial power distribution. Two distinct regimes of DNB exist. The upper (DNB-1) regime shows continuously decreasing DNB heat flux with increasing SEF

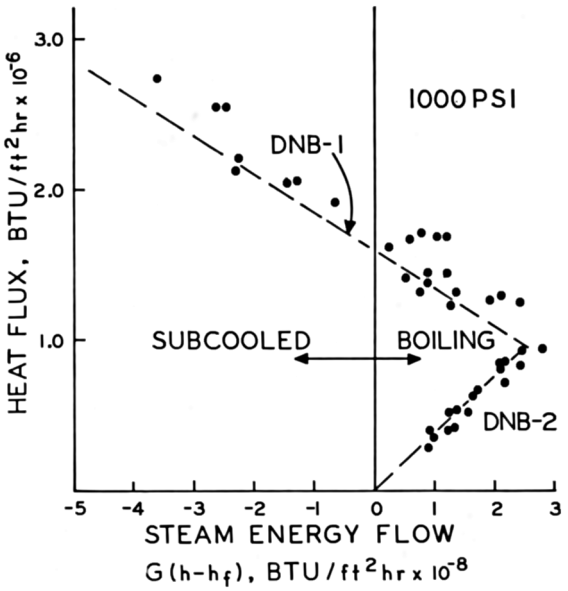

Fig. 1. DNB heat flux vs. steam energy flow at 1000 psi in vertical tubes. Data from WAPD-188 and ANL4627.

through the subcooled region and extending well into the quality region. In this regime the transition from normal boiling into film blanketing is usually a sharp one, and usually occurs at heat fluxes exceeding 0.5×10^6 Btu/ft² hr. Burnout of this type can be considered a *thermal instability*.

A lower-heat-flux (DNB-2) regime exists in channels with net boiling. The data plot along a line which corresponds to a constant ratio of boiling length to thermal equivalent diameter, $L_B/D_Q = (Q/A)/4G(h - h_f)$ and consequently to a constant ratio of boiling length to total length L_B/L_T. The thermal equivalent diameter, $D_Q = 4$ (flow area)/(heated perimeter) is identical to hydraulic diameter when heated and wetted perimeters are identical. Usually,

$$0.8 \leqq (L_B/L_T)_{\text{DNB-2}} \leqq 1.0 \tag{1}$$

Equation (1) signifies that most data obtained with the boiling length greater than 80% of the total length lie in the DNB-2 regime. DNB in this regime has been observed at heat fluxes as low as 10^4 Btu/ft² hr; it is usually accompanied by large oscillations in flow and pressure drop and can be considered a *hydrodynamic instability*.

In each regime high-quality, low-mass-velocity points lie adjacent to low-quality, high-mass-velocity points.

For data in which $L_B/L_T < (L_B/L_T)_{\text{DNB-2}}$, hydrodynamic instabilities are seldom found and points lie in the DNB-1 regime. A simple expression which describes the major trends in DNB-1 data over wide ranges of subcooled and quality operation is:

$$(Q/A)_{\text{DNB-1}} = [(Q/A)_{\text{DNB-1}}]_{h=h_f} - \frac{G(h - h_f)}{A} \tag{2}$$

To fit data considered here, substitution of empirical constants provides (2a) in the Btu-ft-hr-lb system.

$$(Q/A)_{\text{DNB-1}} = 3.8(h_{fg})^2 - \frac{G(h - h_f)}{400} \tag{2a}$$

$$14.7 \text{ psi} \leqq P \leqq 2750 \text{ psi}.$$

Extrapolation of this correlation to very high steam energy flows is questionable, since available data at high steam energy flow is questionable, since available data at high steam energy flow usually lie on the DNB-2 line. DNB-1 data at high steam energy flow must be obtained with test channels of very large L_T/D_Q, operated at low heat fluxes and with considerable inlet sub-cooling. If more data were available in this region a DNB-1 correlation could be obtained which could be used with confidence even for very long reactors.

Changes in flow-loop and test-channel configuration and in instrumentation used to detect DNB usually exert relatively minor effects on DNB-1 heat flux. Both increasing G and decreasing D_Q tend to produce small increases in $(Q/A)_{DNB-2}$ beyond those implicit in Eq (2).

The DNB-2 curve, however, is highly dependent on the details of the system; in particular, the slope of the DNB-2 curve is inversely proportional to L_B/D_Q. Figure 2 shows correlating curves in the boiling region for a tube and for a rectangular channel heated on both sides, as well as data points for 7-rod and 19-rod bundles. Note that all test points on bundles appear to be in the DNB-2 or oscillating-flow regime, and that the critical L_B/D_Q lies between 70 and 80 for the 19-rod bundle and between 80 and 90 for the 7-rod bundle. These bundles were evidently tested with boiling lengths which were too long to permit nonoscillatory (DNB-1) burnout.

Figure 3 compares experimental data from one apparatus at three pressures with the above equations. The critical boiling length for hydrodynamic instability (DNB-2) is essentially independent of pressure. DNB-1 heat fluxes increase continuously with decreasing pressure.

It appears that one of the major shortcomings of many currently used (and conflicting) DNB correlations is their attempts to write single expressions which include both "normal" DNB-1 data and pulsating-flow DNB-2 data. If DNB vs. SEF plots are used to segregate the two kinds of data, it appears likely that useful correlations of a detailed nature could be obtained which are vastly superior to either

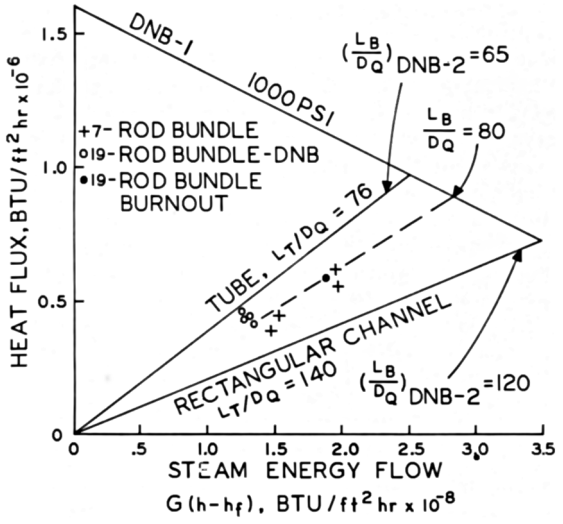

FIG. 2. DNB-1 and DNB-2 heat flux vs. steam energy flow for several flow-channel configurations. Data from WAPD-188.

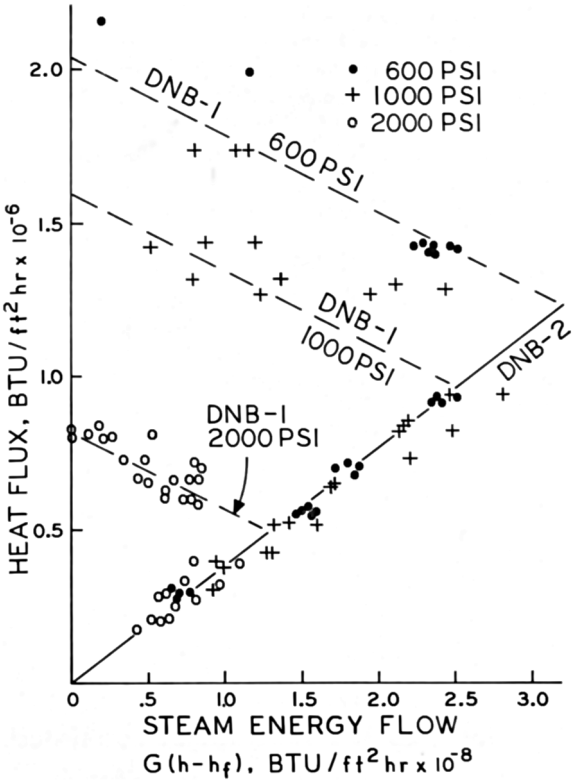

FIG. 3. DNB heat flux data and correlation curves at three pressures. D = 0.306 inches, L_{total} = 23.25 inches. Data from WAPD-188.

the approximations presented here or to the currently-used correlations.

Experimental points in both DNB regimes represent the exit values, or right-hand termini, of horizontal (constant heat-flux) lines which begin at the lower SEF value of the test section inlet. The length of horizontal line representing a test run is equal to the change in SEF from inlet to outlet, and can be calculated from Eq. (3).

$$\Delta\text{SEF} = G(h_{exit} - h_{inlet}) = 4\frac{L_{total}}{D_Q}\left(\frac{Q}{A}\right) \qquad (3)$$

In Fig. 1, for channels with subcooled inlet, the region to the left of the DNB-1 and DNB-2 curves represents the "safe" operating region for uniformly heated sections. Note that under these conditions a maximum exit steam energy flow of about 2.5×10^8 Btu/ft² hr can be obtained from a channel at a heat flux of about 10^6 Btu/ft² hr; an attempt to obtain the same steam flow at *lower* heat flux would result in oscillatory burnout. Thus the concept of using a "burnout ratio" based on the upper, DNB-1, line as a safety factor may not in itself be sufficient to assure conservative design.

Most H_2O and D_2O-cooled reactors operate with design maximum heat fluxes below the DNB-1 range. It appears, therefore, that burnout by the customarily-assumed thermal instability of the DNB-1 mechanism is unlikely except during large reactivity excursions. Burnout in the hydrodynamically-unstable DNB-2 regime appears much more likely, particularly for very long reactors, such as

those designed for D_2O, and it is suggested that more emphasis be placed on the latter phenomenon. The hydrodynamic instability is a strong function of not only L_B/L_T, but also of the configuration of the test section, and of the entire flow loop, pressure drop, and presumably of power distribution. The use of flow-stabilizing orifices presumably increases the critical L_B/L_T, while the existence of compressible volume in the loop may decrease it; in fact, hydrodynamic instabilities can be induced even in the subcooled region if surge volume is present.

WILLIAM J. LEVEDAHL

Martin-Marietta Corp.
Nuclear Division
Baltimore 3, Md.

Received January 25, 1962
Revised March 27, 1962

Minimum Mass Thin Fins with Internal Heat Generation

In a recent paper (*1*) Minkler and Rouleau have considered the effect of a constant heat generation rate (Q Btu/hr-ft^3) on the heat transfer in thin longitudinal fins. In particular, they have asserted that the temperature gradient is constant in a fin designed to have minimum mass (= minimum profile area A_p) in the class of fins which transfer a specified amount of heat (q_0 Btu/hr-ft) from a base at a specified temperature (T_0) by convection to surroundings at another specified temperature (selected as the zero of the temperature scale) if the thermal conductivity k and the heat transfer coefficient h are constant. I have shown elsewhere (*2*) that this assertion is mathematically incorrect when $Q > 0$ (the error is significant only for large Q), and have set up and solved the problem of Bolza in the calculus of variations to find the fin profile and the temperature distribution for the fin with minimum profile area.

Since the optimum fin profile has a sharp tip (this is true also for the optimum fin with a constant temperature gradient) it is natural to inquire what penalty in profile area must be paid in order to use a fin with a triangular profile, as in Fig. 1. This question is answered here, and the results are presented in Fig. 2, which shows a graph of the dimensionless quantity $\alpha = h^2kT_0^3A_p/q_0^3$ versus $\Lambda = Qq_0^2/kh^2T_0^3$ for the optimum triangular fin as well as for the optimum fin and several points for the optimum fin with a constant temperature gradient. The data for the curved fins are taken from ref. *2*. We also show in Fig. 2 graphs of the dimensionless over-all height of the fin $\mu = whT_0/q_0$.

With reference to Fig. 1, let $q(x)$ and $T(x)$ be respectively the heat flow rate per unit length of fin (Btu/hr-ft) and temperature excess over the surroundings at the point x in the fin where the fin thickness (ft) is $2\delta x/w$. Then

$$q(x) = 2k\frac{\delta x}{w}\frac{dT}{dx}, \frac{dq}{dx} = 2hT - \frac{2Q\delta x}{w}, 0 < x < w, \qquad (1)$$

are the differential equations governing the heat transfer in the fin. Since no heat flows through the tip of the fin, we have

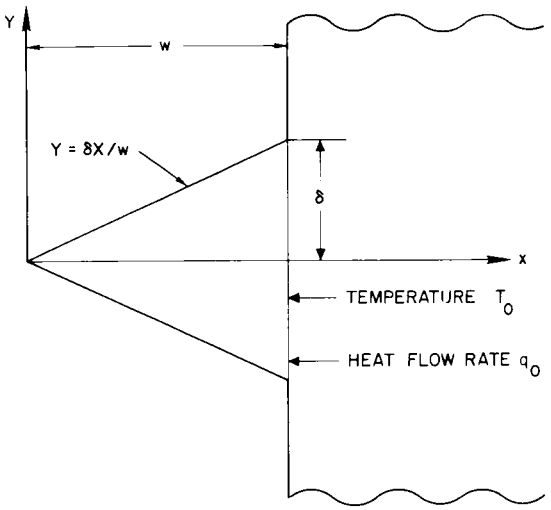

FIG. 1. Sketch of profile of triangular fin

the boundary conditions

$$x = 0, q = 0; x = w, q = q_0, T = T_0. \qquad (2)$$

The fin profile area is

$$A_p = \delta w, \qquad (3)$$

and the mathematical problem is that of finding two constants δ and w and two functions $q(x)$ and $T(x)$, defined when $0 \leqq x \leqq w$, and satisfying the differential equations (1) and the boundary conditions (2), for which the profile area (3) is a minimum.

If we eliminate q from the differential equations (1) and the boundary conditions (2), we see that

$$\frac{d}{dx}\left(x\frac{dT}{dx}\right) = \frac{hwT}{k\delta} - \frac{Qx}{k}, 0 < x < w, \qquad (4)$$

$$x = 0, x\frac{dT}{dx} = 0; x = w, T = T_0, \frac{dT}{dx} = \frac{q_0}{2k\delta}. \qquad (5)$$

A particular solution of the inhomogeneous linear differential equation is $Qk\delta^2/h^2w^2 + Q\delta x/hw$, and the general solution can be found by adding to this particular solution the general solution of the homogeneous linear differential equation. If a new variable $u = 2(hwx/k\delta)^{1/2}$ is introduced, the homogeneous equation takes the form

$$u\frac{d^2T}{du^2} + \frac{dT}{du} - uT = 0$$

of Bessel's equation of zero order and imaginary argument. Therefore the general solution of the differential equation (4) is

$$T = \frac{Qk\delta^2}{h^2w^2} + \frac{Q\delta x}{hw} + T_0[BI_0(u) + CK_0(u)], \qquad (6)$$

in which B and C are arbitrary constants, and I_0 and K_0 are the standard Bessel functions of zero order. In terms of the dimensionless quantities α, Λ, and μ introduced earlier and $\lambda = 2(hw^2/k\delta)^{1/2}$, we see that

$$Q = \frac{kh^2T_0^3\Lambda}{q_0^2}, w = \frac{\mu q_0}{hT_0}, \delta = \frac{4q_0^2\mu^2}{hkT_0^2\lambda^2},$$